# Synthesis and properties of random poly(lactic acid)-based ionomers

Andrew J. Ro [a], Samuel J. Huang [a,b], R.A. Weiss [a,c,*]

[a] Polymer Program, University of Connecticut, Storrs, CT 06269-3136, USA
[b] Dept. of Chemistry, University of Connecticut, Storrs, CT 06269-3136, USA
[c] Dept. of Chemical Engineering, University of Connecticut, Storrs, CT 06269-3136, USA

## ARTICLE INFO

## ABSTRACT

A random poly(lactic acid), PLA, based ionomer was synthesized by copolymerizing a methacrylate-terminated PLA macromonomer and methyl methacrylate. The copolymerization kinetics were studied using ^{1}H NMR spectroscopy and the copolymer composition was characterized by ^{13}C NMR spectroscopy. Carboxylic acid groups were introduced into the copolymer by reacting the hydroxyl end groups of the PLA macromonomer with succinic anhydride, and the acid groups were neutralized with metal acetates to produce Na-, Ca-, and Y-PLA ionomers. Significant increases in $T_g$ were observed for the ionomers and thermomechanical analysis indicated that the ionomers were more resistant to penetration by a weighted probe and an apparent rubbery plateau was observed above $T_g$. The ionomers were more hydrophilic than PLA, but relatively low water absorption could be achieved for the $Ca^{2+}$-salt ionomer.

## 1. Introduction

The disposal of conventional commodity polymers such as polyolefins has become a significant problem in solid waste management [1]. The resistance to biodegradation of petroleum-based polymers has fueled research and development of biodegradable polymers. From 1996 to 2005, the total consumption of biodegradable polymers increased from 14,000 to 85,000 mton, and it is projected that consumption will double by 2010 [1,2]. Poly(lactic acid), PLA, is the only current commodity biodegradable polymer, and the major producer of PLA, NatureWorks, LLC, has a production capacity of 140,000 ton/year [3]. Major applications of PLA include packaging films, fibers, thermoformed containers, and biomedical devices.

The deficiencies that limit the use of PLA are its poor toughness and its low glass transition temperature ($T_g$), ~60 °C, compared to other commodity thermoplastics [4–6]. PLA with at least 85% L-lactide units is a semi-crystalline polyester, but with a slow crystallization rate, and polymers with 15% D-lactic acid units are amorphous and optically clear [7]. Crystallinity increases the softening temperature of PLA and improves its mechanical properties above $T_g$, but the transparency decreases, which makes it unsuitable for packaging and coating applications [4–6]. The toughness of PLA can be improved by orientation [4], blending [8], and copolymerization [9], though none of these approaches are considered a commercially viable solution for applications of PLA requiring higher toughness than the conventional resin.

Predominantly hydrophobic polymers containing a modest amount (e.g., up to 15 mol%) of covalently bonded salt groups, such as metal carboxylates or sulfonates, are referred to as ionomers [10]. The ionic groups tend to form ion-rich, nm-sized aggregates due to dipole–dipole interactions, which act as reversible cross-links. These materials exhibit physical characteristics of a chemically crosslinked polymer, but processability is possible in solution or in the melt at elevated temperatures. The dipolar interactions restrict segmental mobility, which increases $T_g$ of the polymer. The increase in $T_g$ of ionomers often scales as the Coulombic potential energy, $E_c = kq_1q_2/a$, where $k$ = Coulomb's constant = $1/(4\pi\varepsilon_o)$, $\varepsilon_o$ is the dielectric constant of the medium, $q_1$ and $q_2$ are the negative and positive charges and $a$ is the separation of the charges [11]. For a common backbone and anion (e.g., carboxylate), $E_c \propto q/a$, where $q = q_2$, the charge of the cation. Thus, for a fixed charge density, i.e., concentration of salt groups, for a fixed polymer backbone and anion, one expects that $T_g \propto q/a$, and the effect of charge density often follows the scaling rule $T_g \propto cq/a$, where $c$ = the concentration of salt groups.

A number of research groups have previously considered the effects of modifying polyesters with ionic groups. The incorporation of metal-neutralized 5-(sodiosulfo)isophthalate, SSI, groups

* Corresponding author. Polymer Program, University of Connecticut, 97N. Eagleville Rd., Storrs, CT 06269-3136, USA. Tel.: +1 860 486 4698; fax: +1 860 486 6048.
E-mail address: rweiss@mail.ims.uconn.edu (R.A. Weiss).

into poly(ethylene terephthalate), PET, increases $T_g$ and the melt viscosity [12–16]. Other researchers have also used PET ionomers to promote compatibility of polymer blends, enhance dye retention and reduce moisture absorption [17–25]. Vidotti et al. [26] used the PET–SSI ionomers to exfoliate or intercalate organically modified montmorillonite in PET/clay nanocomposites. Sherman and Storey synthesized telechelic polycaprolactone (PCL) and PLA carboxylate ionomers and demonstrated that the introduction of the metal carboxylate groups increased $T_g$ and hindered crystallization [27,28]. Ro et al. [29] recently synthesized ω- and α,ω-metal carboxylate-PLA ionomers using a chemical recycling process and found that $T_g \propto q/a$. A problem with telechelic-PLA ionomers is that the ionic concentration is coupled to molecular weight, so that low molecular weights are necessary to achieve the higher charge densities that provide useful increases of $T_g$. This paper describes the synthesis of random carboxylate-PLA ionomers and their thermal and thermomechanical properties. Incorporation of the ionic groups randomly along the chain allows one to independently vary the molecular weight and the ionic concentration. A goal of the research described herein was to prepare PLA ionomers of higher molecular weight and ionic concentrations than were possible in the previous work on telechelic-PLA ionomers. The higher molecular weight was expected to increase the $T_g$ compared to the relatively low $T_g$s achieved with low molecular weight telechelics and provide molecular entanglements of the chains. The higher carboxylate concentration was expected to provide greater physical crosslinking, i.e., higher crosslink density, and greater improvements in $T_g$ and the mechanical properties than was the case with the telechelic ionomers.

## 2. Experimental

### 2.1. Materials

PLA with an $M_n = 65,000$ g/mol and $M_w = 121,000$ g/mol (as determined by gel permeation chromatography using polystyrene standards) was obtained from Cargill Corp. (now NatureWorks, LLC) and was dried in a vacuum oven at 70 °C under reduced pressure for 12 h. 1,4-Dioxane (Fisher Scientific Inc., 99%) was distilled over sodium and benzophenone prior to use. Chloroform (CHCl$_3$, J.T. Baker Inc. PHOTREX reagent, 99.8%) was distilled over calcium hydride at 70 °C and 2-hydroxyethyl methacrylate (HEMA, Sigma Chemical Co., 97%) was distilled under reduced pressure. Succinic anhydride (SA, Aldrich Chemical Co., 97%) was recrystallized in CHCl$_3$ and washed with ethyl ether. The purified product was filtered and dried in a vacuum oven at 25 °C under reduced pressure for 6 h. Methyl methacrylate (MMA, Fisher Scientific Inc., 99%) was dried over CaH$_2$ (Acros Organics Co) and passed through a basic Al$_2$O$_3$ column. 2,2′-Azobis(2-methylpropionitrile) (AIBN, Aldrich Chemical Co., 98%) was recrystallized in methanol. All other reagents were used without further purification. A 0.0649 M stock solution of hydroquinone (HQ, Sigma Chemical Co. ≥99%) was prepared in 1,4-dioxane. Tin(II) 2-ethylhexanoate (SnOct, ∼95%), trichloroacetyl isocyanate (TAI, 96%), and calcium acetate were purchased from Sigma Chemical Co. Yttrium(III) acetate hydrate and 1-methylimidazole (NMIM, 99+%) were purchased from Aldrich Chemical Co. Methanol, sodium acetate and potassium acetate were purchased from Fisher Scientific Inc. Dimethylformamide (DMF), zinc acetate dihydrate, and lithium acetate were purchased from Acros Organics Co.

### 2.2. Materials' characterization

Nuclear magnetic resonance, NMR, experiments were done on a Bruker DRX-500 MHz using 5 mm o.d. sample tubes. $^1$H NMR spectra were collected from solutions in deuterated chloroform (CDCl$_3$, Cambridge Isotope Laboratories, Inc.) containing 1% tetramethylsilane, TMS, as an internal reference. $^{13}$C NMR spectra were acquired using sample concentrations of 16.7% (w/v) in CDCl$_3$ (Cambridge Isotope Laboratories, Inc., 99.8%). An inverse gated decoupling $^{13}$C NMR experiment was performed using a delay time (D1) of 10 s, in order to ensure the complete relaxation of all carbon nuclei. Inverse gated decoupling $^{13}$C NMR was used to obtain reliable quantitative intensities by eliminating the nuclear Overhauser effect and differences in carbon relaxation rates exhibited in broad band-decoupling NMR [31].

FTIR spectra were measured with a Nicolet Magna IR 560 spectrometer using pellets prepared from KBr powder (Fisher Scientific Inc. 99.9%). Each sample was analyzed with 128 scans with 2 cm$^{-1}$ resolution. Fourier self-deconvolution and peak fitting were performed using GRAMS/AI software (Galactic Industries, Salem, NH). Fourier self-deconvolution narrows the trace bandwidth features, which aids in identifying the overlapping, principal bands that comprise the more complex spectrum [32]. This type of deconvolution can be used for an accurate determination of the number of peaks in a trace region, the band positions, and areas under the peak. An exponential filter was used to sharpen the spectral features. Fourier self-deconvolution tends to increase the apparent noise in the data, so a low pass smoothing filter was also used. After the self-deconvolution, peak fitting was performed with the spectra using a Lorentzian function with a linear baseline.

Thermal properties were analyzed with a TA Instruments Q100 differential scanning calorimeter, DSC, using heating and cooling rates of 20 °C/min between −30 °C and 170 °C. Samples were sealed in aluminum pans and experiments were run under an argon atmosphere. The previous sample thermal history was removed by heating the sample to 170 °C for 5 min and then quenching to −30 °C before the thermal analyses. Temperatures and enthalpies were calibrated using an indium standard.

Thermomechanical analysis, TMA, was performed with a TA Instruments Q400 Thermomechanical Analyzer. A penetration probe with a force of 70 mN was applied to the samples while they were heated from 10 °C to 250 °C at the rate of 10 °C/min. The samples were prepared by compression molding the ionomers into films at 180 °C on a Carver Press, model 2731, and a pressure of 1.1 MPa. The molten films were quenched to room temperature and cut into 5 × 5 mm squares that were 1.3–1.8 mm thick.

Solution viscosity measurements were done with a Brookfield DV-II+ PRO viscometer utilizing a small sample adapter. Samples were prepared by dissolving the polymer in a DMF/methanol (15:1 v/v) solvent mixture. Viscosity was measured at 25 °C at shear rates ranging from 79.2 to 178.2 s$^{-1}$.

Water sorption measurements were made by submerging rectangular samples (ranging from 29.2 mm$^2$ to 36.6 mm$^2$ in surface area) in distilled, deionized water. The thickness of the samples ranged from 0.95 to 1.71 mm. After the samples were submerged for 24 h, they were removed from the water and weighed after patting the surface with a laboratory tissue.

### 2.3. Synthesis of α-methacryloyl-ω-hydroxyl PLA (HPLA)

Wallach and Huang [30] previously described the synthesis of methacrylate-terminated PLA (HPLA). In this study, we used a "chemical recycling" process to synthesize the PLA macromonomer, which involved a transesterification reaction of a commercial PLA with 2-hydroxyethyl methacrylate, HEMA. SnOct was used to catalyze the transesterification reaction, during which the PLA was depolymerized to a targeted molecular weight. Wallach and Huang [30] reported that this process produced

a macromonomer with higher polydispersity and lower optical purity than a macromonomer prepared from ring-opening polymerization. The chemical recycling process is a relatively facile method to produce PLA macromonomers compared to ring-opening polymerization, because purification of the precursors is not required for the preparation of the reaction. In this study, the targeted molecular weight of the macromonomer was $M_{macro} = 500$ g/mol, which provided a reasonable reactivity, solubility, and diffusivity in the reaction mixture.

All glassware and the stir-blade were dried in an oven at 160 °C and allowed to cool over $CaSO_4$ in a dessicator. PLA (100 g) was melted under a $N_2$ purge at 190 °C in a 250 mL flask equipped with a mechanical stirrer. The flask was then charged with HEMA (27.89 mL, 0.231 mol) and SnOct catalyst (2% w/w PLA). The reaction mixture was heated and stirred at 190 °C for 2 h to reduce the molecular weight of the PLA and functionalize one end of it with HEMA, see Scheme 1(A). The reaction flask was then quenched in cold water and the HEMA-functionalized polymer was dissolved in $CHCl_3$ (20% w/v, 500 mL final volume). The catalysts and other byproducts were extracted by washing the organic solution twice with 10% aqueous HCl (500 mL) and twice with distilled, deionized water (500 mL). The organic layer was dried with anhydrous $MgSO_4$ and the solvent was removed by vacuum distillation. The product was dried in a vacuum oven at 60 °C for 24 h.

$^1$H NMR ($CDCl_3$) $\delta$ (ppm): 1.4–1.7 [15H, br, $CH_3$, lactic acid], 1.9 [3H, s, $CH_3$, methacrylate], 4.3 [4H, br, $CH_2CH_2$, ethyl methacrylate], 5.1–5.2 [5H, br, CH, lactic acid], 5.6 and 6.1 [2H, s, $CH_2$, methacrylate].

### 2.4. Copolymerization of HPLA and methyl methacrylate

The copolymer precursors (**COPOLY**) were prepared by copolymerizing the PLA macromonomer, with methyl methacrylate, MMA (Scheme 1) (B). HPLA (60 g, 0.114 mol), MMA (13.0 mL, 0.122 mol), AIBN (0.402 g, mol), and 518 mL of 1,4-dioxane were added to a 1000 mL one-neck round bottom flask. The reaction mixture was degassed with three freeze–pump–thaw cycles and filled with $N_2$. The reaction proceeded at 65 °C in an oil bath for 48 h. The solvent was removed by vacuum distillation and the polymer was then dried in a vacuum oven at 60 °C for 24 h.

IR ($cm^{-1}$): 3509 (OH), 2997 and 2953 (CH stretch), 1761 (C=O stretch).

### 2.5. Kinetic study of copolymerization

HPLA (2 g, 3.80 mmol), MMA (0.435 mL, 4.08 mmol), AIBN (13.4 mg, mmol) and 25 mL of 1,4-dioxane were added to a 50 mL Schlenk tube. The reaction mixture was degassed with 3 freeze–pump–thaw cycles and filled with $N_2$. The copolymerization reaction was carried out at 65 °C in an oil bath for 48 h. Samples (0.37 mL) were periodically extracted under $N_2$ using an airtight syringe and 0.14 mL of HQ solution was added to each of the samples to quench the reaction. The conversion and copolymer molecular weight of each sample were measured using GPC and NMR, where HQ was used as an internal reference.
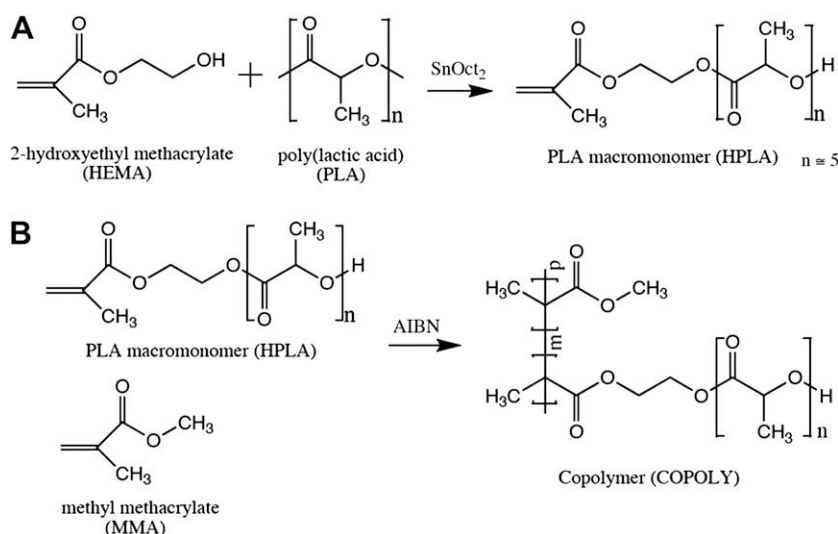
### 2.6. Carboxylic acid-functionalized copolymer (COPOLYSA)

COPOLY (20 g), succinic anhydride, SA (0.655 g, 6.55 mmol), and 1-methylimidazole, NMIM (0.401 mL) were dissolved in $CHCl_3$ (250 mL), see Scheme 2. The reaction was performed in a one-neck, 500 mL round bottom flask with a condenser. The reaction solution was refluxed at 75 °C for 20 h. The organic layer was then washed twice with 10% aqueous HCl (250 mL) and twice with distilled and deionized water (250 mL). The solvent was removed from the organic layer by vacuum distillation and then dried in a vacuum oven at 60 °C for 24 h. Note that in the product copolymer, the carboxylic acid groups are located at the free ends of the PLA macromonomer branched chains. The ion-exchange capacity (IEC) was 0.69 meq/g, as determined by end group analysis from $^1$H NMR spectroscopy.

IR ($cm^{-1}$): 3503 (OH and COOH), 2997 and 2953 (CH stretch), 1760 (C=O stretch).

### 2.7. Metal carboxylate ionomer (COPOLYSA-M, where M is the metal counter ion)

COPOLYSA (15 g) was dried in a vacuum oven at 60 °C for 24 h and then neutralized to various degrees at 180 °C with an appropriate amount of metal acetate for 15 min under vacuum in a 250 mL round bottom flask equipped with a mechanical stirrer. The reaction mixture was cooled by quenching the flask in dry ice. The samples prepared are summarized in Table 1. The nomenclature used for the ionomers was COPOLYSA-Mx, where M denotes the metal counter ion and x = the percent neutralization of the carboxylic acid groups.



**Scheme 1.** Synthesis of (A) the PLA macromonomer (HPLA) and (B) MMA and PLA macromonomer copolymer (COPOLY).
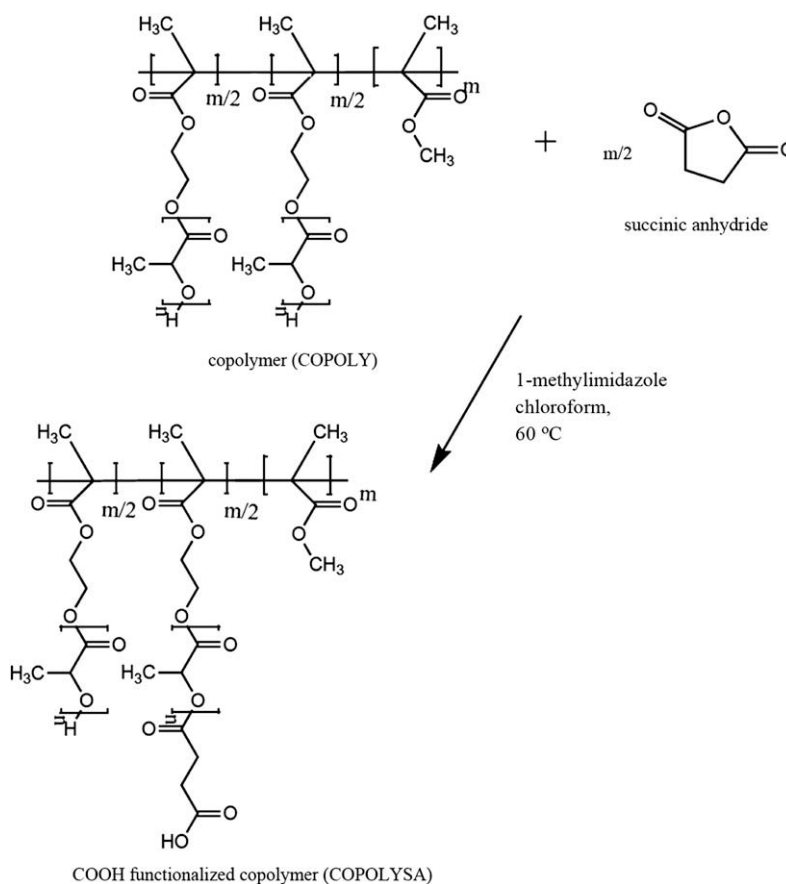
**Scheme 2.** Reaction of copolymer (COPOLY) with succinic anhydride to produce carboxylic acid-functionalized copolymer (COPOLYSA).

## 2.8. Trichloroacetyl isocyanate, TAI, derivatization of COPOLY

The COPOLY sample (10 mg) was dried in a vacuum oven at 60 °C for 24 h and then dissolved in $CDCl_3$ (0.5 mL). An excess amount of TAI (~0.1 g) was added to the solution and the dissolved sample was then transferred to an NMR tube for $^1H$ NMR spectrum analysis.

## 3. Results and discussion

### 3.1. Macromonomer

The number-average molecular weight ($M_n$) of the HPLA was 500 g/mol, as determined by end group analysis using $^1H$ NMR

**Table 1**
Sample characteristics. The IEC of the COPOLYSA was 0.69 meq/g.

| Sample | M | [COO⁻] mmol/g | Neutralization (%) | $T_g$ (°C) |
|---|---|---|---|---|
| COPOLY | – | – | – | 40 |
| COPOLYSA | $H^+$ | 0 | 0 | 43 |
| COPOLYSA-Na29 | $Na^+$ | 0.20 | 29 | 51 |
| COPOLYSA-Na58 | $Na^+$ | 0.40 | 58 | 56 |
| COPOLYSA-Na87 | $Na^+$ | 0.60 | 87 | 57 |
| COPOLYSA-Na100 | $Na^+$ | 0.69 | 100 | 56 |
| COPOLYSA-Ca29 | $Ca^{2+}$ | 0.20 | 29 | 53 |
| COPOLYSA-Ca58 | $Ca^{2+}$ | 0.40 | 58 | 55 |
| COPOLYSA-Ca87 | $Ca^{2+}$ | 0.60 | 87 | 58 |
| COPOLYSA-Ca100 | $Ca^{2+}$ | 0.69 | 100 | 56 |
| COPOLYSA-Y29 | $Y^{3+}$ | 0.20 | 29 | 54 |
| COPOLYSA-Y58 | $Y^{3+}$ | 0.40 | 58 | 52 |
| COPOLYSA-Y87 | $Y^{3+}$ | 0.60 | 87 | 52 |
| COPOLYSA-Y100 | $Y^{3+}$ | 0.69 | 100 | 54 |

spectroscopy. That was calculated from the ratio of the integrations of the peaks that corresponded to the vinyl protons of the methacrylate moiety and the methine proton of the lactic acid repeat unit. The polydispersity of the macromonomer was 1.3 as measured by GPC.

### 3.2. Copolymerization of MMA and PLA macromonomer

The reactivity ratios $r_{MMA}$ and $r_{HPLA}$ for the copolymerization of MMA and HPLA were calculated from the kinetic study described above. The conversion of the monomers was calculated from the consumption of the vinyl groups using $^1H$ NMR spectroscopy. The ratio of vinyl groups remaining at each reaction time was calculated from the integrated areas of the 5.58 ppm peak for the MMA and the 5.62 ppm peak for the HPLA, see Fig. 1. Using the known concentration and proton integration of hydroquinone, the concentration of the consumed vinyl groups was determined from the integrations of the vinyl protons, Fig. 1. The reaction kinetics, plotted in Fig. 2, indicated that the MMA and HPLA monomers were consumed at similar rates. The reactivity ratios $r_{MMA} = 0.46$ and $r_{HPLA} = 0.63$ were calculated using the Kelen–Tudos method [33–35]. The relative reactivity ratios showed that the monomers preferentially reacted with each other and they exhibited a moderately ideal copolymerization behavior. Based on the kinetics of the vinyl group consumption from the $^1H$ NMR spectra and the integrations from the $^{13}C$ NMR spectrum, the composition should be relatively close to the monomer feed.

An MMA and HPLA copolymer was synthesized on a larger scale using a molar feed ratio of [MMA]/[HPLA] = 1.07. The copolymer equation [33–35] using the reactivity ratio values given above
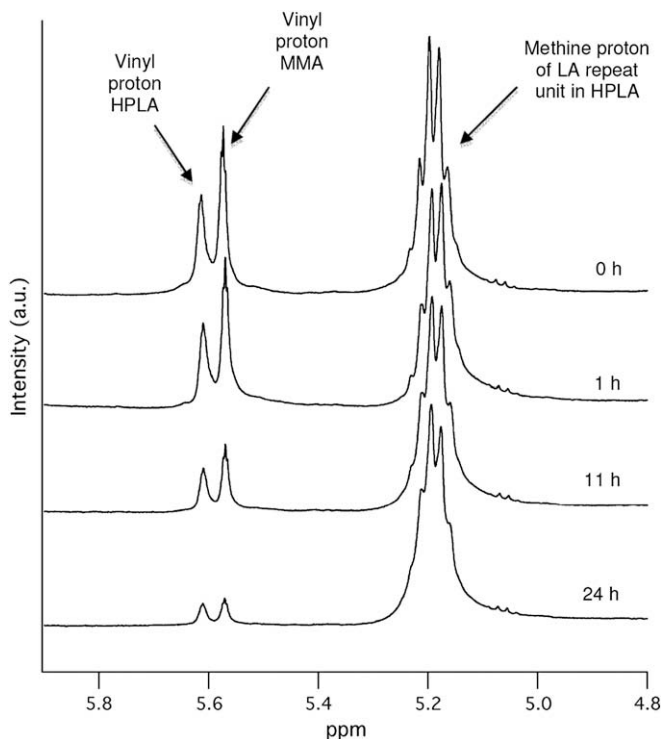
**Fig. 1.** ^{1}H NMR spectra of samples extracted from a copolymerization of MMA and HPLA at various times during the reaction.

predicts that the copolymer product should have an average composition within about 10% of a 50/50 and the copolymer should be somewhat alternating. The conversion of the large-scale copolymerization was 97%. The composition of the copolymer was 50/50 MMA/HPLA, as determined from the ratios of the integrated peak intensities corresponding to the two species measured by inverse gated decoupling ^{13}C NMR spectroscopy (Fig. 3). That composition corresponds to a molar and mass ratio of MMA/LA of 1/5 and 5/18, respectively. The copolymer had an $M_n = 36,000$ g/mol, as determined by GPC.

### 3.3. Carboxylic acid functionalization

The conversion of the hydroxyl groups in COPOLY to carboxylic acid groups is shown in Scheme 2. The targeted amount of hydroxyl
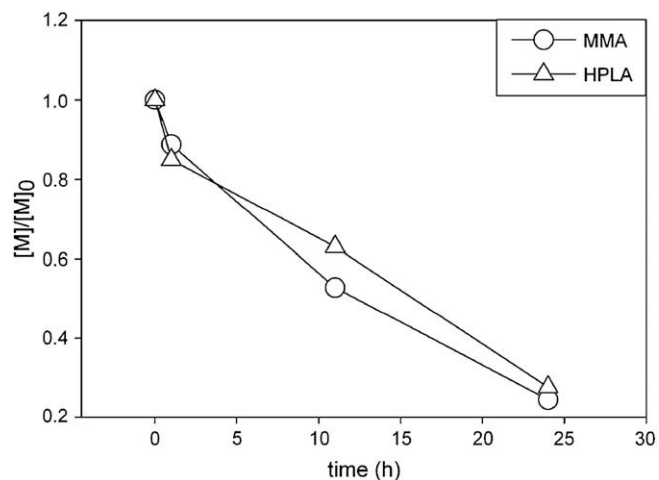


**Fig. 2.** Conversion of MMA and PLA macromonomer in copolymerization reaction over 24 h period.

groups for this reaction was 50% (see Section 2 for details), which corresponds to IEC = 0.85 meq/g, or a 1:1:10 ratio of hydroxyl:-carboxyl:lactic acid units. The determination of the amount of carboxyl and hydroxyl groups was necessary to calculate the reaction efficiency of the carboxylic acid functionalization and the ion-exchange capacity. The concentrations of carboxyl and hydroxyl groups were quantified using the derivatization method described by Donovan and Moad [36]. The derivatization method involves reacting TAI with the hydroxyl and carboxyl functional groups to produce two different imides, which exhibit characteristic N–H resonances that can be distinguished and analyzed by ^{1}H NMR. Donovan and Moad reported that TAI reacted quantitatively with the hydroxyl and carboxyl groups in a number of polyesters. The NH resonance resulting from the carboxyl group reacting with TAI [C(O)–O–C(O)–NH–C(O)CCl$_3$] should occur between $\delta = 10$ and 11.5 ppm, and the NH product of the reaction with the hydroxyl groups [O–C(O)–NH–C(O)CCl$_3$] should show up between $\delta = 8$ and 9 ppm [36]. The ratio of the integrated area under those peaks corresponds to the ratio of hydroxyl and carboxyl group concentrations.

The ^{1}H NMR spectra of the derivatized COPOLY and COPOLYSA are shown in Fig. 4. The broad peak at 8.5–9.1 ppm in the COPOLY is due to the imide proton derived from the reaction of TAI with the hydroxyl groups of the copolymer. After functionalization of COPOLY with succinic anhydride, a sharp peak is seen at 10.3 ppm due to the imide proton derived from the reaction of TAI with the carboxyl groups. A broad resonance at 8.5–9.1 ppm also remains due to unreacted hydroxyl groups. The extraneous resonance at 9.7 ppm may be from unidentified byproducts resulting from the TAI derivatization. The integrations of the hydroxyl and carboxyl resonances indicated that the succinic acid reaction efficiency was 80%, and the actual ratio of hydroxyl:carboxyl:lactic acid units in COPOLYSA was 0.67:1:10. The IEC was 0.69 meq/g.

The carboxylic acid groups in COPOLYSA were analyzed by FTIR spectroscopy. The band assignments were based on the work of Coleman et al. on poly(ethylene-co-methacrylic acid) ionomers [37]. The strong absorption band at ~1760 cm$^{-1}$ present in all the spectra is due to the carbonyl stretching of the methacrylate and PLA repeat units. The carbonyl stretching vibration of the non-hydrogen bonded carboxylic acid should be at 1750 cm$^{-1}$ and the hydrogen bonded dimer form should be found at 1700 cm$^{-1}$. These peaks were not readily visible in the COPOLYSA spectrum due to the overlapping peaks. Deconvolution and peak fitting were performed on the FTIR spectra in order to resolve these peaks. The deconvoluted spectra of COPOLY and COPOLYSA are shown in Fig. 5. Both spectra show the stretching bands from the ester carbonyl groups at 1730 and 1760 cm$^{-1}$, which correspond to the carbonyl groups from the lactic acid and methacrylate repeat unit. These carbonyl groups exhibit slightly different stretching bands depending on the various inter- and intramolecular environments. Upon functionalizing the copolymers with succinic anhydride, the deconvoluted spectrum of COPOLYSA shows the stretching band of the non-hydrogen bonded carboxylic acid at 1700 cm$^{-1}$ and the hydrogen bonded dimer stretching at 1780 cm$^{-1}$. Peak fitting was performed on the deconvoluted peaks using a Lorentzian line shape with an offset baseline. The spectral subtraction between the experimental COPOLYSA spectrum and the deconvoluted spectrum exhibited minimal differences.

Neutralization of the COPOLYSA was confirmed by the appearance of a broad absorption band between 1500 and 1650 cm$^{-1}$ in the salt derivatives, which is due to the carbonyl stretching from the metal carboxylate groups (Fig. 6). Fourier self-deconvolution was employed on the ionomer spectra in order to resolve the carboxylic acid and carboxylate absorbances (Fig. 7). The Fourier self-deconvolution was applied to all of the spectra in the same
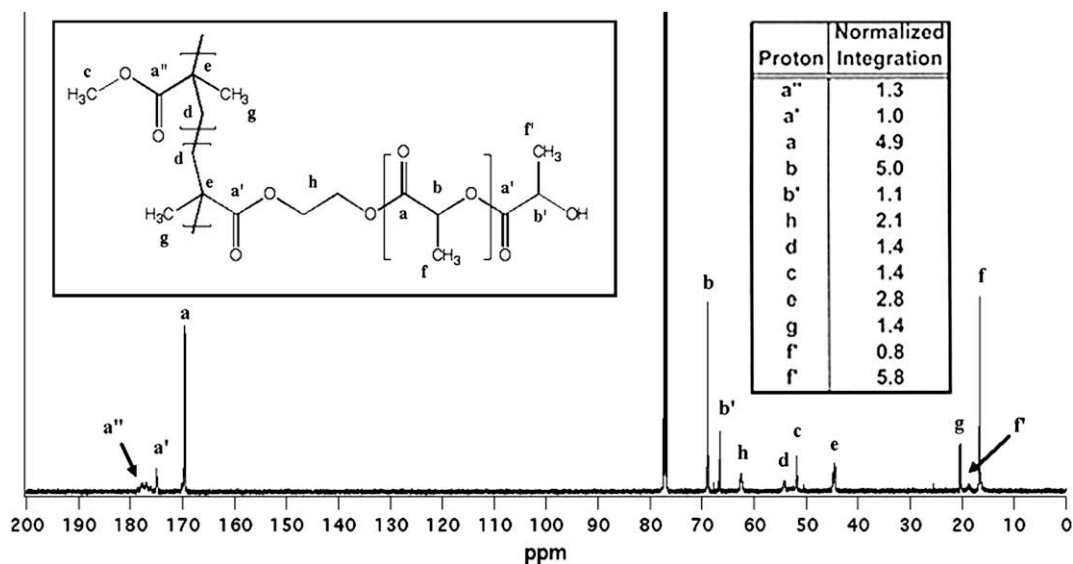
**Fig. 3.** $^{13}$C NMR spectrum of COPOLY obtained from inverse gated decoupling experiment.

way. The exponential deconvolution filter was used to the same extent to resolve and sharpen spectral features and a smoothing filter was used minimally in order to reduce the noise. The peak areas of these absorbances can be used to determine the degree of neutralization. The deconvolution did not yield any absorbances from the carbonyls of hydrogen bonded and non-hydrogen bonded carboxylic acid groups that are found at 1700 and 1780 cm$^{-1}$. The lack of carboxylic acid bands in the deconvoluted ionomer spectra suggests that the neutralization reaction reached complete conversion for all the ionomers.

### 3.4. Thermal analysis

All the polymers and ionomers prepared in this study were completely amorphous. Their $T_g$s as determined by DSC are summarized in Table 1. The $T_g$ of COPOLY was 40 °C and increased to 43 °C upon incorporation of the carboxylic acid functionality. That small increase is most likely due to the intermolecular hydrogen bonding of the carboxylic acid groups. Conversion of the COPOLYSA to the Na$^+$, Ca$^+$ or Y$^{+3}$-salts further increased $T_g$. The effect of the
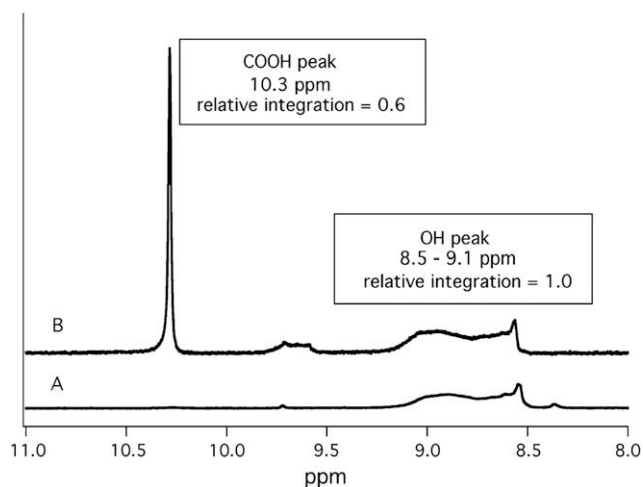


**Fig. 4.** Determination of hydroxyl and carboxyl concentration of COPOLYSA using derivatization method with trichloroacetyl isocyanate (TAI): $^1$H NMR spectra of the derivatized (A) COPOLY and (B) COPOLYSA.

degree of neutralization on the $T_g$ for the different metal carboxylates is shown in Fig. 8. The conversion of acid groups to salt groups increased $T_g$ from 8 to 15 °C, depending on the counter-ion used and the extent of neutralization. Only a single sample was used to determine the $T_g$s of the ionomers, so the differences between the values for the different salts may be due, at least in part, to experimental errors in the $T_g$s. But, it is clear that a substantial increase of $T_g$ from the value of 43 °C for the acid derivative, COPOLYSA, occurs within the first 20% of neutralization for each salt. After that, the $T_g$ may either increase (as seen with the Na- and Ca-salts) or remain relatively constant. More data are needed to definitively substantiate any trend with respect to the effects of the counter ion and higher neutralization.

It is clear from the data in Fig. 6, however, that respectable increases in the $T_g$ of the PLA copolymers can be realized by conversion of the acid to a salt. This is a consequence of the stronger intermolecular dipole–dipole interactions of the ion pairs compared to hydrogen bonding, which suppresses segmental mobility of the ionomer. Based on a previous study of telechelic ionomers [29], it was expected that the $T_g$ would scale with the Coulomb energy of the ion pair, $\sim q/a$, which in this case increases for the different cations as Na$^+$ < Ca$^{2+}$ < Y$^{3+}$, but that prediction is not confirmed by the data in Fig. 8. Also, multivalent counter ions, such as Ca$^{+2}$ and Y$^{+3}$, can produce intermolecular dipolar interactions of ion pairs (if the cation is shared by two anions on the same chain) or ionic bonds (if a single cation is shared by anions on different chains), which one might expect would be more efficient at suppressing segmental mobility. However, the data in Fig. 8 suggest that the distinction of the type of intermolecular bonding on $T_g$ is important in these ionomers.

In order to confirm that the increases of $T_g$ of the ionomers were due to the presence of the metal carboxylate groups, another COPOLY sample was exposed to the same reaction conditions used to make the ionomers, without the carboxylic acid functionalization step. This included adding equivalent amounts of metal acetate to the COPOLY and washing the product in the same way as the COPOLYSA-M samples. The resulting materials exhibited no change in $T_g$.

### 3.5. Thermomechanical analysis

TMA penetration profiles of the COPOLYSA-M100 ionomers, COPOLYSA and COPOLY are shown in Fig. 9. The
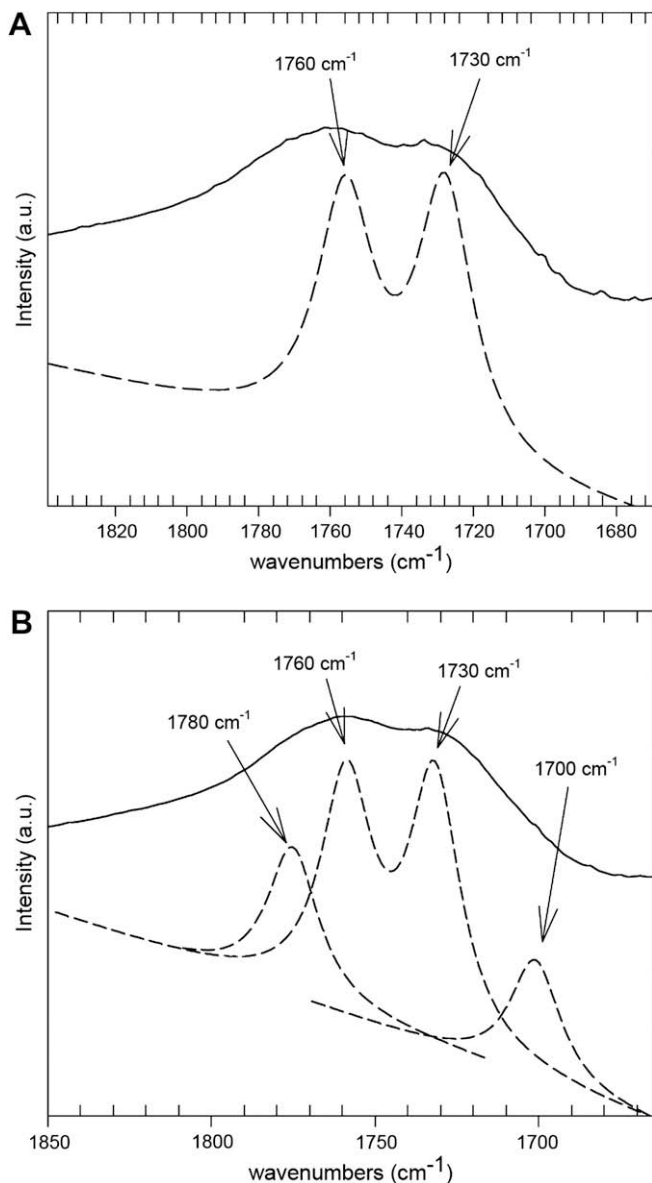
**Fig. 5.** FTIR spectra of (A) COPOLY and (B) COPOLYSA (solid lines) and its deconvoluted spectra using a Lorentzian function (dashed lines).

hydroxyl-terminated COPOLY and the acid derivative COPOLYSA showed similar softening behavior, where immediately above $T_g$, the TMA probe penetrated through the samples at similar rates. In contrast, above $T_g$, the TMA probe only penetrated ~30 to 40% into the ionomers. The constant value of penetration with time is reminiscent of the rubbery plateau that is usually observed for cross-linked elastomers. Similar behavior is also usually observed for ionomers, where the dipole–dipole interactions behave as physical crosslinks. No viscous flow, i.e., complete penetration of the sample, was observed for any of the COPOLYS-M100 ionomers up to 200 °C. And, no clear effect of the counter-ion used is observed from the data in Fig. 9.

Most random ionomers exhibit nanophase separation of ion-rich aggregates, called ionic clusters, as a result of the incompatibility of the ionic groups and the hydrophobic matrix polymer. Evidence for that phenomenon is the observation of a peak corresponding to a characteristic size of 1–5 nm in the structure factor measured by small angle X-ray scattering. However, no SAXS peak was observed in the SAXS data (*not shown*) obtained for these
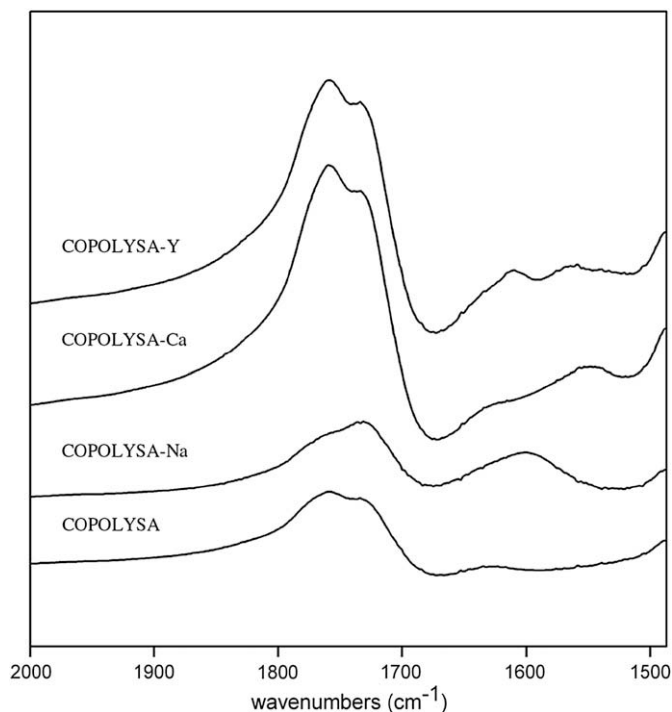


**Fig. 6.** FTIR spectra of COPOLYSA and its various metal salts.

ionomers. This indicates that the ionic "order" in these highly branched ionomers is noticeably different than that in other random ionomers. However, the limited mechanical data, shown in Fig. 7, indicate that even without the nanophase separation of ionic clusters, the "crosslink" structure of these materials is rather effective at suppressing softening and viscous flow of these ionomers.

### 3.6. Solution viscosity

The COPOLY and COPOLYSA polymers were soluble in chloroform, tetrahydrofuran (THF), and dimethylformamide (DMF). PMMA is known to be soluble in xylene and toluene but the ionomers were insoluble in aromatic hydrocarbons. Solvents such as chloroform, tetrahydrofuran, or DMF swelled the ionomers, but the addition of a more polar protic solvent, such as methanol, was needed to dissolve the ionomers. Even in that case, the solubility was limited. A 15:1 DMF/methanol mixed solvent system was used to dissolve 1 g of ionomer in 16 mL of the mixed solvent system and the percentages that were soluble are listed in Table 2.

The solubility behavior of the COPOLYSA-M polymers was typical of ionomers. That is, the ionomer does not dissolve in a solvent for the parent polymer as a result of the persistence of the ionic interactions that occur in a relatively low dielectric constant solvent. The low dielectric constant solvent may be able to solvate the non-ionic part of the ionomer, but a more polar solvent is needed to breakup the ionic associations. The solubility of the ionomers increased as the valency of the cation increased, see Table 2, which is counter-intuitive, since the higher valency ions formed stronger ion pairs (i.e., higher $q/a$). Of course, the molar concentration of the different cations for a fixed polymer concentration and IEC is different, i.e., $[Na^+] = 0.69$ mmol/g, $[Ca^{2+}] = 0.35$ mmol/g, and $[Y^{3+}] = 0.23$ mmol/g, so the different solubilities may be related to the coordination stoichiometry between the methanol and the cation, though that was not measured in this study.
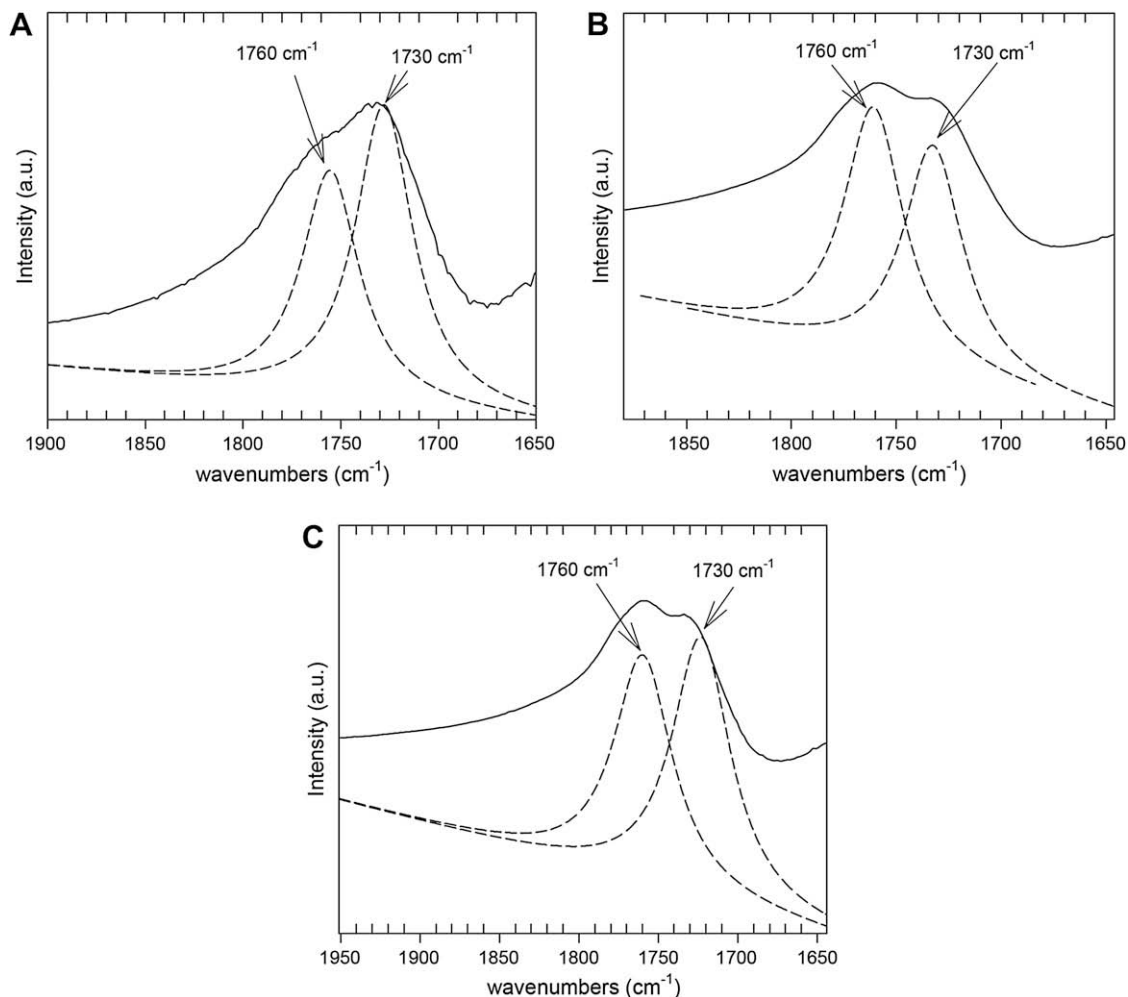
**Fig. 7.** FTIR spectra of the PLA-based ionomers containing (A) Na, (B) Ca, and (C) Y salts. The deconvoluted spectra using a Lorentzian function are shown as dashed lines.
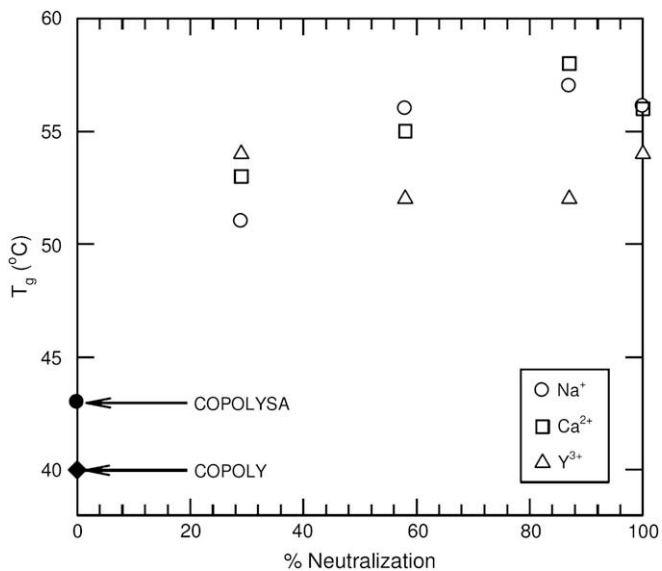
The dilute solution viscosities of COPOLY, the ionomers (COPO-LYSA-M100), and their acid derivatives (COPOLYSA) in a 15:1 DMF/methanol mixed solvent system are shown in Fig. 10. The introduction of carboxylic acid groups (i.e., COPOLYSA vs. COPOLY) increased the viscosity by ∼19%. The viscosities of the $Ca^{2+}$- and



**Fig. 8.** $T_g$ of the COPOLYSA-M ionomers as a function of neutralization level. The IEC of the parent COPOLYSA was 0.69 meq/g.
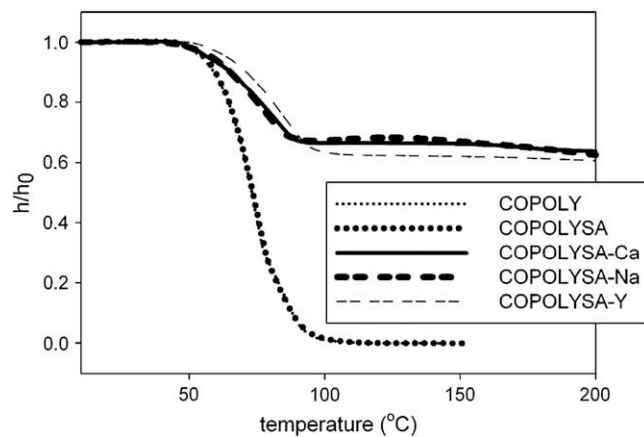


**Fig. 9.** TMA penetration porfiles for COPOLY, COPOLYSA, and the COPOLYSA-M100 ionomers. $h_0$ is the sample thickness and $h$ is the instantaneous position of the penetration probe.

**Table 2**
The solubility of the ionomers in a 15:1 DMF/methanol solvent system.

| Ionomer | Ionomer dissolved (g/dL) | % Soluble in DMF/methanol |
|---------|--------------------------|---------------------------|
| Na      | 2.94                     | 47                        |
| Ca      | 4.01                     | 64                        |
| Y       | 4.50                     | 72                        |

**Table 3**
Water sorption of COPOLY, COPOLYSA, and COPOLYSA-M100 expressed by increase in weight %.

| Sample        | wt%  | Hydration number |
|---------------|------|------------------|
| COPOLY        | 1.8  | –                |
| COPOLYSA      | 3.3  | 2.6              |
| COPOLYSA-Na100| 52.8 | 42.5             |
| COPOLYSA-Ca100| 3.4  | 5.5              |
| COPOLYSA-Y100 | 11.1 | 26.9             |

$Y^{3+}$-salts were similar to those of COPOLYSA at the lower concentrations, but became significantly higher at the higher concentrations as shown in Fig. 10. The viscosities of the $Na^+$-salt were lower than the COPOLYSA and the other ionomers and comparable to COPOLY. One would expect dipole–dipole interactions of the Na-carboxylate groups to increase the viscosity in a similar manner as for the $Ca^{2+}$- and $Y^{3+}$-salts, but that clearly was not the result – at least at the low concentrations for which the Na-carboxylate data were obtained. A possible explanation for this is that where only intermolecular dipole–dipole interactions were possible (e.g., Na-carboxylate), the methanol co-solvent effectively solvated those interactions, so that all intermolecular interactions in solution were suppressed. In the case of the $Ca^{2+}$- and $Y^{3+}$-salts, as discussed above, intermolecular ionic bonds (e.g., $R–COO^-–M^{++}–^-OOC–R$, where $R$ = the rest of the polymer chain) can occur in addition to dipole–dipole interactions, and it is unlikely that methanol would breakup the ionic bond.

### 3.7. Water sorption

Table 3 lists the equilibrium water absorption of the polymers used in this study. The incorporation of carboxylic acid groups into the COPOLY increased the water sorption, as a result of the addition of hydrogen bonding sites. The water absorption of the $Na^+$- and $Y^{3+}$-salts was significantly greater than that of the COPOLYSA, which is a consequence of the hydration properties of the cation. The water absorbance of COPOLYSA-Ca100 was much lower compared to that of COPOLYSA. Again, this is a consequence of the poor water hydration of Ca-carboxylates [38]. Since PLA degrades hydrolytically, the water content of the polymer is important, and these data indicate that for an ionomer, the water content can be controlled by the choice of the counter ion. For example, the $Ca^{2+}$-salt of an ionomer with an ionic concentration of 0.69 meq/g had an equilibrium water content of only 3.3 wt%, compared to 1.8 wt% for the non-ionic polymer. Alternatively, the water content can be

increased $\sim 15$ times by switching the salt from $Ca^{2+}$ to $Na^+$, as a consequence of the different hydration properties of the cation.

Previous studies have shown that the overall hydration number and the degree of ionic dissociation are important factors in adsorption [38,39]. The approximate hydration numbers (the number of water molecules per ion) for dissolved $Na^+$, $Ca^{2+}$, and $Y^{3+}$ ions are shown in Table 3. The overall hydration of polymers containing carboxylates with alkaline earth metals is reported to be less than that for alkali metal salt [38,40], which is consistent with the results shown in Table 3. No data was found for hydration of polymer containing Y-carboxylate or other group 3 metal ions. The sorption trend may also be dependent on the molar concentration of the different cations, i.e., $[Na^+] = 0.69$ mmol/g, $[Ca^{2+}] = 0.35$ mmol/g, and $[Y^{3+}] = 0.23$ mmol/g. The Na ionomer has the highest metal ion concentration, thus more water can be absorbed.

## 4. Conclusions

Random ionomers based on a predominantly poly(lactic acid), PLA, polymer can be easily prepared by a chemical recycling process that involves transesterification of a commercial PLA. The introduction of metal carboxylate groups increases $T_g$, 11–18 °C for an IEC = 0.69 meq/g, depending on the choice of the cation. $T_g$ can also be controlled by varying the fraction of carboxylic acid groups that are converted to metal carboxylate. The choice of the cation influenced the properties above $T_g$, and converted the material from a viscous liquid to a rubbery material above $T_g$. An increase in the elasticity of the melt is a consequence of strong intermolecular dipole–dipole interactions. These interactions also persist in solution, which also raises the solution viscosity. Although the ionomers absorb more water than does unmodified PLA, the amount of water absorbed can be controlled with the choice of the cation. In general, the introduction of ionic functional groups into PLA offers the opportunity to vary and control the softening behavior, rheology, mechanical properties, transport properties and biodegradation behavior.

Although the ionic groups did improve the $T_g$ of the non-ionic, modified PLAs, the $T_g$s of the modified PLAs were still considerably lower than that of neat, high molecular weight PLA. Thus, the modification used herein is not particularly useful for improving the absolute value of the $T_g$ of PLA. The modification, however, does improve the resistance of PLA to softening above $T_g$, and that has practical value even if $T_g$ is relatively low. And, the addition of the polar functionality may provide improvements in compatibility of PLA with other polymers and provide improved adhesion to other materials. Those aspects of the PLA ionomers deserve future consideration. The low $T_g$ is most likely due to the flexible groups used in the preparation of the macromonomer. Future studies will be directed at identifying different chemistries that will not decrease the PLA $T_g$ when it is modified. Also, further studies to understand the relationship between the counter-ion valency and the size with $T_g$ and a more detailed study of the microstructure should be carried out.
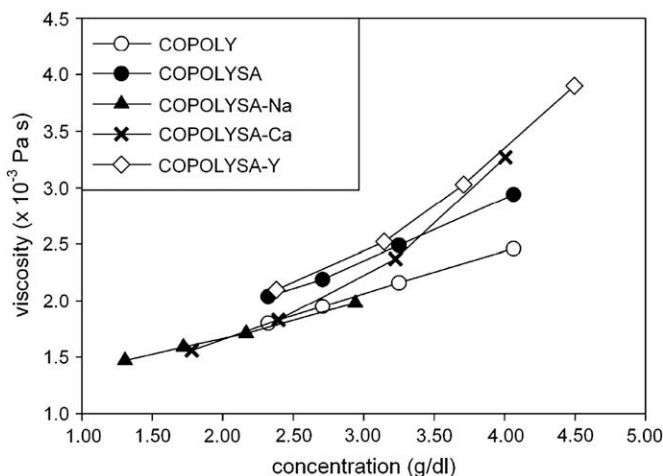


**Fig. 10.** The viscosity as a function of concentration (g/mL) for COPOLY, COPOLYSA, and the PLA-based ionomers.

## References

[1] Municipal solid waste generation, recycling, and disposal in the United States: facts and figures for 2006. U.S. Environmental Protection Agency; 2006.
[2] Schlechter M. Biodegradable polymer (Report P-175). Norwalk: Business Communications Company; 2001.
[3] Trembley JF. Chem Eng News 2007;85:41.
[4] Sinclair RG. J Macromol Sci Part A Pure Appl Chem 1996;33(5):585–97.
[5] Lipinsky ES, Sinclair RG. Chem Eng Prog 1986;82:26–32.
[6] Mobley DP. Plastics from microbes: microbial synthesis of polymers and polymer precursors. Ohio: Hanser Gardner Publications; 1994.
[7] Bigg DM. An Tech Conf Soc Plast Eng 1996;54(2):2028–39.
[8] Chen X, Schiling K, Kelly W. US Patent 5,756,651; 1998.
[9] Spinu M, Jackson C, Keating M, Gardner K. J Macromol Sci Pure Appl Chem 1996;A33:1497.
[10] Tant MR, Mauritz KA, Wilkes GL, editors. Ionomers: synthesis, structure, properties and applications. London: Blackie Academic Press; 1997.
[11] Eisenberg A. Macromolecules 1971;4:125–8.
[12] Kang H, Long TE. Polyme Mater Sci Eng 2001;84:909–10.
[13] He H, Liang B, Wang Q. Zhongguo Fangzhi Daxue Xuebao 1998;24(2):17–21.
[14] Guo X-Y, Gu L-X, Feng X-X. J Appl Polym Sci 2002;86(14):3660–6.
[15] Greener J, Gillmor JR, Daly RC. Macromolecules 1993;26(24):6416–24.
[16] Connelly RW, McConkey RC, Noonan JM, Pearson GH. J Polym Sci Polym Phys Ed 1982;20(2):259–68.
[17] Iyler S, Schiraldi DA. J Polym Sci Part B Polym Phys 2006;44(15):2091–103.
[18] Gemeinhardt GC, Moore AA, Moore RB. Polym Eng Sci 2004;44(9):1721–31.
[19] Yoo E-S, Farris RJ. PMSE Prepr 2004;90:462–3.
[20] Sunderland NJ, Hein CL, Dhawan S. Eur Pat Appl 1318176; 2003.
[21] Kim BC, Nguyen VK, Jeong MY, Lee DS. Polym J (Tokyo, Jpn) 2003;35(1):79–83.
[22] Bastiaens JHP, Carminati A. PCT Int Appl WO 2002033000 A2; 2002.
[23] Boykin TL, Moore RB. Polym Eng Sci 1998;38(10):1658–65.
[24] Ng C-WA, Macknight WJ. Macromolecules 1994;27(11):3033–8.
[25] Hsieh KH, Pan JP, Chen LW, Frisch KC. Adv Urethane Sci Technol 1987; 10:77–83.
[26] Vidotti SE, Chinellato AC, Hu G-H, Pessan LA. J Polym Sci Part B Polym Phys 2007;45(22):3084–91.
[27] Sherman JW, Storey RF. Polym Prepr (Am Chem Soc Div Polym Chem) 1998;39(2):602–3.
[28] Sherman JW, Storey RF. Polym Prepr (Am Chem Soc Div Polym Chem) 1999;40(2):952–3.
[29] Ro AJ, Huang SJ, Weiss RA. Polymer 2008;49:422–31.
[30] Wallach JA, Huang SJ. ACS Symp Ser 2000;764:281–92.
[31] Mitchell TN, Costisella B. NMR – from spectra to structures. Germany: Springer Verlag; 2004. p. 26.
[32] Griffiths PR, Pariente G. Trends Anal Chem 1956;5:209–15.
[33] Kelen T, Tudos F. React Kinet Catal Lett 1974;1:487.
[34] Kelen T, Tudos F. J Macromol Sci Chem 1975;A9:1.
[35] Kelen T, Tudos F. Makromol Chem 1990;191:1863.
[36] Donovan AR, Moad G. Polymer 2005;46:5005–11.
[37] Lee YJ, Painter PC, Coleman MM. Macromolecules 1988;21:346–54.
[38] Brozoski BA, Painter PC, Coleman MM. Macromolecules 1984;17:1591–4.
[39] Berthold J, Rinaudo M, Salmen L. Colloids Surf A Physicochem Eng Asp 1996;112:117–29.
[40] Zundel G. Hydration and intermolecular interactions. New York: Academic Press; 1969.